

High precision Zernike modal gray map reconstruction for liquid crystal corrector

This article has been downloaded from IOPscience. Please scroll down to see the full text article.

2010 Chinese Phys. B 19 064214

(<http://iopscience.iop.org/1674-1056/19/6/064214>)

View [the table of contents for this issue](#), or go to the [journal homepage](#) for more

Download details:

IP Address: 221.8.12.150

The article was downloaded on 11/09/2012 at 04:07

Please note that [terms and conditions apply](#).

High precision Zernike modal gray map reconstruction for liquid crystal corrector*

Liu Chao(刘超)^{a)b)†}, Mu Quan-Quan(穆全全)^{a)b)}, Hu Li-Fa(胡立发)^{a)},
Cao Zhao-Liang(曹召良)^{a)}, and Xuan Li(宣丽)^{a)}

^{a)}State Key Laboratory of Applied Optics, Changchun Institute of Optics, Fine Mechanics and Physics,
Chinese Academy of Sciences, Changchun 130033, China

^{b)}Graduate School of the Chinese Academy of Sciences, Beijing 100049, China

(Received 21 October 2009; revised manuscript received 7 November 2009)

This paper proposes a new Zernike modal gray map reconstruction algorithm used in the nematic liquid crystal adaptive optics system. Firstly, the new modal algorithm is described. Secondly, a single loop correction experiment was conducted, and it showed that the modal method has a higher precision in gray map reconstruction than the widely used slope method. Finally, the contrast close-loop correction experiment was conducted to correct static aberration in the laboratory. The experimental results showed that the average peak to valley (PV) and root mean square (RMS) of the wavefront corrected by mode method were reduced from 2.501λ ($\lambda = 633$ nm) and 0.610λ to 0.0334λ and 0.00845λ , respectively. The corrected PV and RMS were much smaller than those of 0.173λ and 0.048λ by slope method. The Strehl ratio and modulation transfer function of the system corrected by mode method were much closer to diffraction limit than with slope method. These results indicate that the mode method can take good advantage of the large number of pixels of the liquid crystal corrector to realize high correction precision.

Keywords: liquid crystal device, adaptive optics, modal gray map reconstruction

PACC: 4270D, 4278F, 6130, 4290

1. Introduction

The adaptive optics system (AOS) can sharpen an image through actively compensating wavefront aberration, and has been widely used in astronomical observation and retinal imaging.^[1–6] The wavefront corrector (WFC) is a key element of the AOS. Universally, deformable mirrors (DMs) are used for this purpose. When a unit voltage is applied to one actuator on DM, the surface deformation produced by this activated actuator is called the actuator's influence function. In a DM AOS, the influence function is usually the slope response measured from the wavefront sensor (WFS), due to the fact that only some elements of the influence function around the actuator's position have non-zero slope values. The slope method in DM AOS is more direct and flexible.^[7]

A nematic liquid crystal (NLC) corrector WFC is an alternative selection for AOS due to its high resolution, high response speed, low cost, reliability, low power consumption, low price and lack of moving mechanical components.^[8–10] It has millions of pixels,

which makes it possible to use phase-wrapping technique to increase modulation depth and also to acquire high correction precision. Also, because of the corrector's large number of pixels, it is impossible to apply a unit voltage on each of the pixels to measure influence function. So, a gray map of a certain Zernike mode is used to drive all pixels of the corrector for influence function measurement. In most current NLC AOSs, the slope method is used.^[11–13] It is clear that nearly all elements of the influence function have non-zero slope values, which may limit the correction precision of the NLC AOS. The peak to valley (PV) and root mean square (RMS) of the wavefront corrected by this kind of system reduced from aberrations of several wavelengths to 0.1λ – 0.2λ and 0.05λ – 0.1λ , respectively.^[11,13] It has a long way to go to reach high precision correction, especially for the open-loop correction which demands a very high correction accuracy.^[14] In addition, after the correction with slope method, we found that the Zernike polynomial coefficients of the residual wavefront did not fluctuate around zero, and different Zernike co-

*Project supported by the National Natural Science Foundation of China (Grants Nos. 60736042, 60578035 and 50703039) and Science and Technology Cooperation Project between Chinese Academy of Sciences and Jilin Province (Grant No. 2008SYHZ0005).

†Corresponding author. E-mail: liuchao678@163.com

© 2010 Chinese Physical Society and IOP Publishing Ltd

<http://www.iop.org/journals/cpb> <http://cpb.iphy.ac.cn>

efficients fluctuated around a different fixed non-zero value. This would decrease the correction precision, and must be avoided. In all, it is very important to improve the control algorithms of the AOS to get high correction precision.

In this paper, we first introduce the measurement of influence function and the gray map reconstruction algorithm of the NLC AOS using slope method, and analyse the precision in Section 2. In Section 3 we propose a new mode algorithm which is special for NLC AOS to measure influence function and reconstruct the gray map, which gets nearly perfect results. Finally, in Section 4 an experiment of a static wavefront correction was conducted in the laboratory. The PV and RMS of the residual wavefront corrected by mode method is only ten percent of that corrected by slope method. The system with the new algorithm becomes closer to the diffraction limit, and the image quality improves obviously.

2. Gray map reconstruction by slope method

In order to correct distortions precisely, a kinoform calculated with high precision called a gray map

must be obtained. The reconstruction of a gray map needs aberrations measured by WFS and influence matrix which is constructed by repeating the influence function measurement on all effective Zernike modes. Most currently used NLC AOS are using the slope method to measure the influence matrix and distortions,^[9,11–13] and we call this kind of system the slope based nematic-liquid-crystal adaptive optical system (SNLC AOS). Next, we introduce the gray map reconstruction algorithm.

2.1. Algorithm

The gray map applied on NLC WFC is represented by Zernike polynomial coefficients a_j ($0 \leq j \leq M$) in reconstruction procedure. The wavefront is calculated according to the following equation

$$\Phi = \sum_{j=1}^M a_j Z_j, \quad (1)$$

where Z_j is the j -th Zernike polynomial.^[15] After the wavefront Φ is quantified by 2π , the gray map is obtained. The relationship of gray map coefficients A , influence matrix C and slope distortion vector K is described below

$$\begin{bmatrix} c_{1,1} & \dots & c_{1,j} & \dots & c_{1,M} \\ \vdots & \ddots & & & \vdots \\ c_{i,1} & & c_{i,j} & & c_{i,M} \\ \vdots & & & \ddots & \vdots \\ c_{N,1} & \dots & c_{N,j} & \dots & c_{N,M} \\ c_{N+1,1} & \dots & c_{N+1,j} & \dots & c_{N+1,M} \\ \vdots & \ddots & & & \vdots \\ c_{N+i,1} & & c_{N+i,j} & & c_{N+i,M} \\ \vdots & & & \ddots & \vdots \\ c_{2N,1} & \dots & c_{2N,j} & \dots & c_{2N,M} \end{bmatrix} \begin{bmatrix} a_1 \\ \vdots \\ a_j \\ \vdots \\ a_M \end{bmatrix} = \begin{bmatrix} k_{1,x} \\ \vdots \\ k_{i,x} \\ \vdots \\ k_{N,x} \\ k_{1,y} \\ \vdots \\ k_{i,y} \\ \vdots \\ k_{N,y} \end{bmatrix}, \quad CA = K, \quad (2)$$

where N is the number of lenslets of Shack–Hartmann WFS (SH WFS), M is the total Zernike mode number (usually it takes the value of 35), $k_{i,x}$ and $k_{i,y}$ represent the slopes of the i -th lenslets of WFS in x and y directions, respectively. Before correction, the influence matrix C has to be measured according to the following procedure: first, the gray map of each

Zernike mode with an appropriate coefficient is applied on NLC WFC. Second, the slopes of wavefront modulated by the NLC WFC are measured, normalized and recorded. Third, the above two steps are repeated for each Zernike mode to obtain the influence matrix. After that, a pseudo-inverse of the influence matrix C^+ called the control matrix can be calculated.

During WFC, the gray map coefficients A are obtained according to the following equation:

$$A = C^+ K. \quad (3)$$

Then the gray map for correction can be calculated from A through Eq. (1).

2.2. Precision of the gray map reconstruction based on slope method

We conducted a close-loop correction experiment for static distortion using SNLC AOS. The results are shown in Fig. 1. Figures 1(a) and 1(b) show Zernike mode coefficients of tilt and defocus mode, respectively. They show that the distortions decreased gradually in the first several loops, and then balanced on a fixed value. Different Zernike coefficients fluctuated around a different fixed non-zero value.

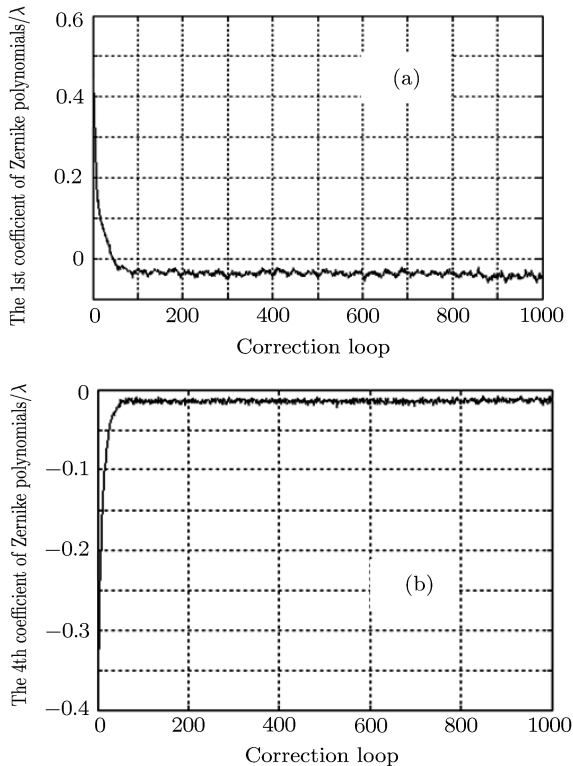


Fig. 1. The dynamic variation of the 1st Zernike coefficient (a) and the 4th Zernike coefficient (b) of the residual wavefront using slope method in LC AOS ($\lambda = 633 \text{ nm}$).

In order to find out the reason why the SNLC AOS yields an abnormal residual error, a single loop correction experiment was conducted. First, after the influence matrix was acquired, the gray map of each Zernike mode with a unit coefficient was sent to NLC WFC, and the slope of the wavefront yielded by the NLC WFC was detected by a WFS. Second,

the Zernike coefficients of the reconstructed gray map were calculated by Eq. (3). Figure 2 gives the reconstructed gray map coefficients after applying the gray map of the 19th or 28th Zernike mode on NLC WFC. In ideal conditions, the gray map coefficients reconstructed from Eq. (3) are the same as the ones that are applied on the WFC. But the fact is that the reconstructed coefficients are not exactly the same as the ones applied on the NLC WFC. In Fig. 3(a) the 19th term of the reconstructed coefficient has a little difference from 1, and other terms that must be zeros have different values. After applying a different gray map of another Zernike mode (not the 19th) on NLC WFC, the reconstructed gray map coefficient profile is nearly the same as that in Fig. 3(a). This gives a good answer to the fact that the residual error does not fluctuate around zero. It proves that the slope method borrowed from DM AOS to reconstruct the gray map has larger than expected error. So the mode method to reconstruct the gray map is under consideration, and we call this kind of system the mode based NLC AOS (MNLCAOS).

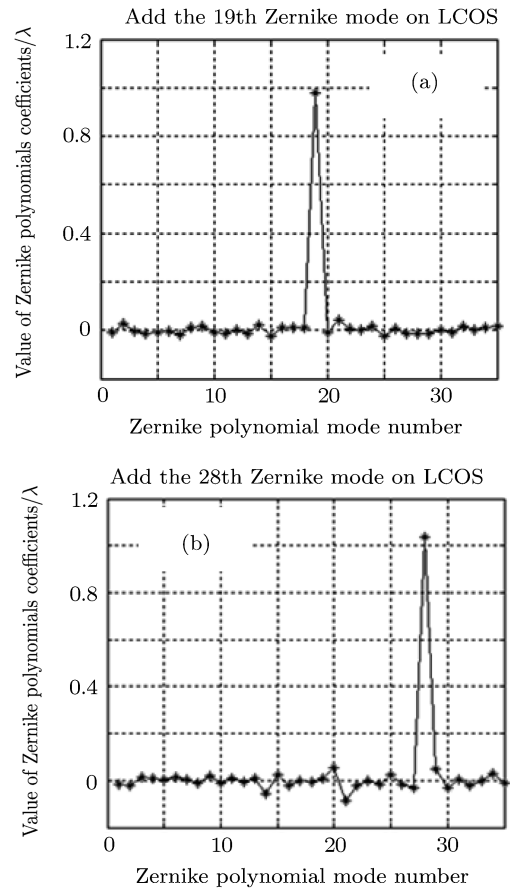


Fig. 2. The Zernike coefficients of the reconstructed gray map by slope method after the gray map of the 19th Zernike mode (a) or 28th Zernike mode (b) were applied on NLC WFC.

3. Gray map reconstruction by mode method

In NLC AOS, the influence function is measured by applying a gray map of a certain Zernike mode on NLC WFC. So it is more reasonable to use mode method to describe the influence function and aberrations.

The influence function measurement of the mode method is similar to that of the slope method. The only difference is that a Zernike coefficient vector is measured and recorded for every Zernike mode. For an aberration which has a series of coefficients d_j ($1 \leq j \leq M$), the reconstructed gray map coefficients c_j ($1 \leq j \leq M$) can be calculated by

$$\begin{bmatrix} c_1 \\ \vdots \\ c_j \\ \vdots \\ c_M \end{bmatrix} = \begin{bmatrix} b_{1,1} & \cdots & b_{1,j} & \cdots & b_{1,M} \\ \vdots & \ddots & & & \vdots \\ b_{i,1} & & b_{i,j} & & b_{i,M} \\ \vdots & & & \ddots & \vdots \\ b_{M,1} & \cdots & b_{M,j} & \cdots & b_{M,M} \end{bmatrix}^{-1} \begin{bmatrix} d_1 \\ \vdots \\ d_j \\ \vdots \\ d_M \end{bmatrix}, \quad C = B^{-1}D, \quad (4)$$

where $b_{i,j}$ is the mode influence matrix element of the i -th Zernike coefficient for the j -th Zernike mode.

The single loop correction experiment was also conducted by using MNLC AOS. The gray map coefficients reconstructed from Eq. (4) are nearly the same as the coefficients of the gray map applied on NLC WFC as shown in Figs. 3(a) and 3(b) by dot lines. For instance, using the MNLC AOS, when the gray map of the 19th Zernike mode was applied on NLC WFC, we found that the 19th reconstructed Zernike coefficient is equal to 1, and others are all zero as shown in Fig. 3(a) by the dotted line, which is more accurate than that using the SNLC AOS as shown in Fig. 3(a) by the star marker line. The results of all M Zernike modes prove that the mode method for the reconstructed gray map is more accurate than that of the slope method in the NLC AOS.

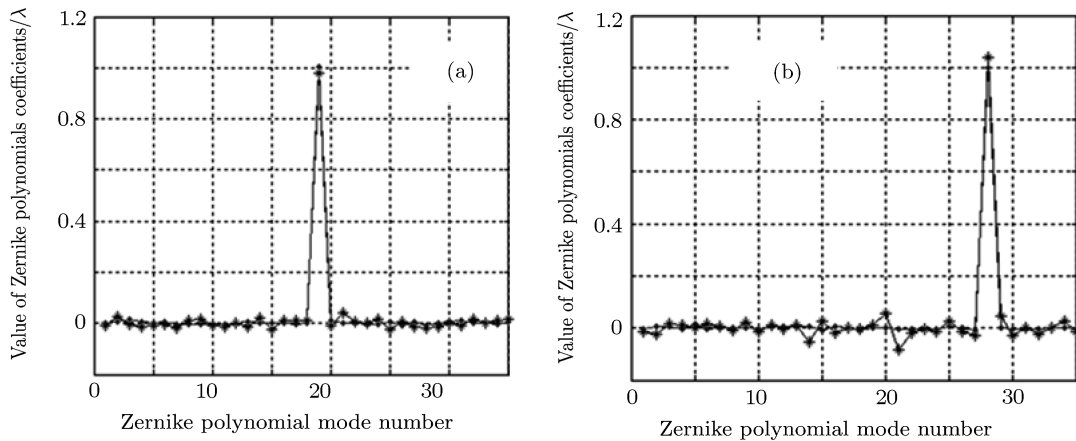


Fig. 3. The reconstructed gray map coefficients using SNLC AOS (star points) or using MNLC AOS (small dot point) after the gray map of the 19th (a) or the 28th (b) Zernike mode were applied on the NLC WFC.

4. Contrast experiment using SNLC AOS and MNLC AOS

In order to compare the correction effects of the SNLC AOS and MNLC AOS, an experiment of a static WFC was conducted in the laboratory. The NLC WFC used in the experiment has 512×512 pixels, a 200-Hz frame rate, and a 1λ ($\lambda = 633$ nm) phase modulation depth. The SH WFS has 415 effective lenslets with a hexagonal arrangement, a 3-mm aperture, and a 500-Hz frame rate. The CCD for imaging the fibre bundle has a 34-Hz frame rate, and 512×512 pixels with a pixel size of $15 \mu\text{m}$. The host computer has a CPU of Intel Core 2 2.66 GHz with 2 GB DDR2 memory.

The experimental setup is shown in Fig. 4. A white light from the fibre bundle passes through a 633-nm narrow-band (about 10 nm) coloured filter and a polarizer to become a near monochromatic p polarized light. After collimating by the lens L1 with a focal length of 300 mm and reflecting by the mirror M1, the light goes

into the NLC WFC. The modulated light is reflected by the NLC WFC along the incident direction. When it meets the beam splitter, it is separated from the incident light. After it goes through a quarter-wave plate, it becomes circularly polarized light. The polarisation beam splitter separates the incident circularly polarized light into s and p polarized light. The s polarized light is collimated by the lens L2 with a focal length of 100 mm, and goes to the SH WFS being used to detect the aberrations. The p polarized light is reflected by a mirror M2, and goes to the CCD camera being used to image the fibre bundle.

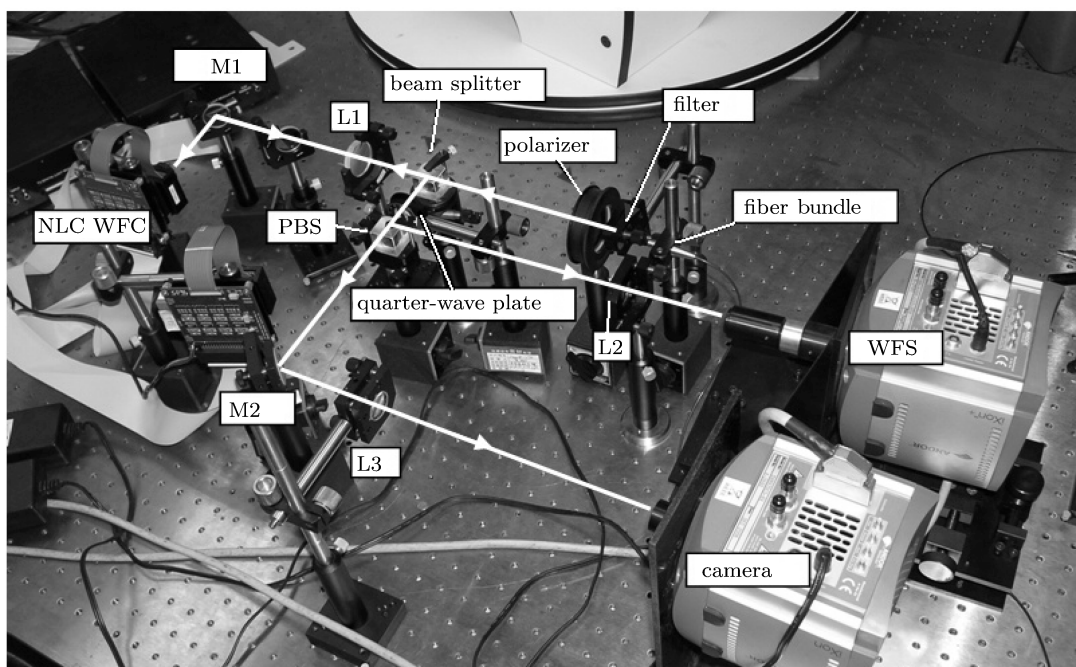


Fig. 4. The setup of NLC AOS.

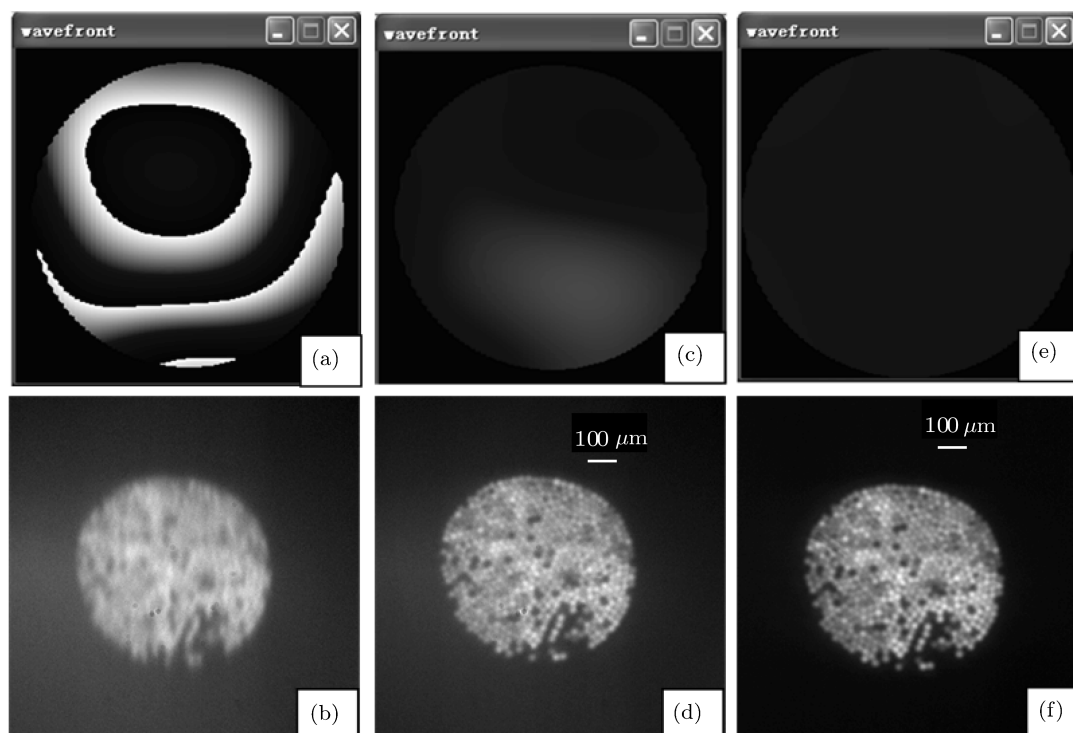


Fig. 5. The aberration wavefront and the image of the fibre bundle: (a), (b) before correction; (c), (d) after the correction of SNLC AOS; (e), (f) after the correction of MNLC AOS.

Before correction, PV and RMS of the wavefront were 2.501λ ($\lambda = 633 \text{ nm}$) and 0.610λ , respectively, as shown in Fig. 5(a). The image of the fibre bundle is shown in Fig. 5(b). The main aberration of the wavefront was defocused, and the image of the fibre bundle was very obscure. After the correction of SNLC AOS, the results were shown in Figs. 5(c) and 5(d). The PV and RMS of the residual wavefront were down to 0.173λ and 0.048λ , respectively. The wavefront became flat and the image became clearer than that before correction. The core of the fibre could be resolved. However, the wavefront still had a relatively big error, and the core of the fibre bundle was still blurry. So the MNLC AOS was used to correct the same wavefront aberration. The results were shown in Figs. 5(e) and 5(f). In this case, the PV and RMS of the residual wavefront were down to 0.0334λ and 0.00845λ , which were nearly one order of magnitude smaller than the ones using SNLC AOS. The wavefront became flatter, and one could hardly find any fluctuation. The contrast of the image was improved and the core of the fibre bundle could also clearly be resolved.

It can be seen from Fig. 6 that, after the correction of SNLC AOS and MNLC AOS, the average RMS of the wavefront changes from 0.610λ to 0.048λ and 0.008λ , respectively. It is obvious that the correction precision of the mode method is higher than that of slope method.

In order to evaluate the image quality of SNLC AOS and MNLC AOS quantitatively, the point spread function (PSF) and the modulation transfer function

(MTF) are given in Figs. 7 and 8, respectively.

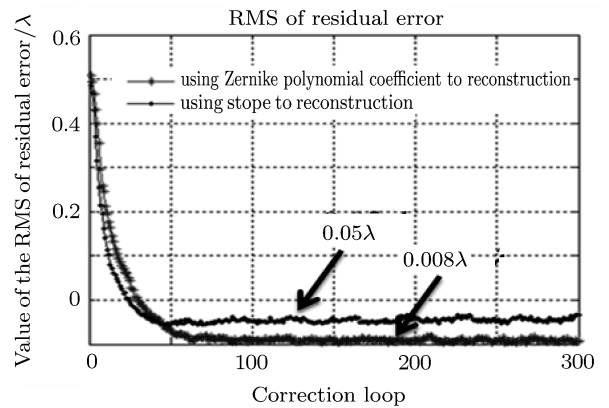


Fig. 6. The dynamic RMS of the residual wavefront after the correction of SNLC AOS (0.05λ) and after the correction of MNLC AOS (0.008λ).

Before correction, the Strehl ratio (SR) was 7.4%. After correction, the SR was up to 93.3% and 99.8% using the SNLC AOS and MNLC AOS, respectively. This is the reason why the image quality with mode method is better. The MTF curves are shown in Fig. 7 before or after WFC. Before correction, it can be seen that the MTF curves of the system have a long distance from the diffraction limit, which suggests that the system has a big aberration. After the correction of SNLC AOS, the difference was smaller (Fig. 7(b)). In Fig. 8(c), we show the MTF curves of the system after correction of MNLC AOS. As can be seen, the match of MTF with diffraction limit was good. The difficulty in identifying the two lines in each plot of Fig. 8(c) indicates the high precision of the mode method in NLC AOS.

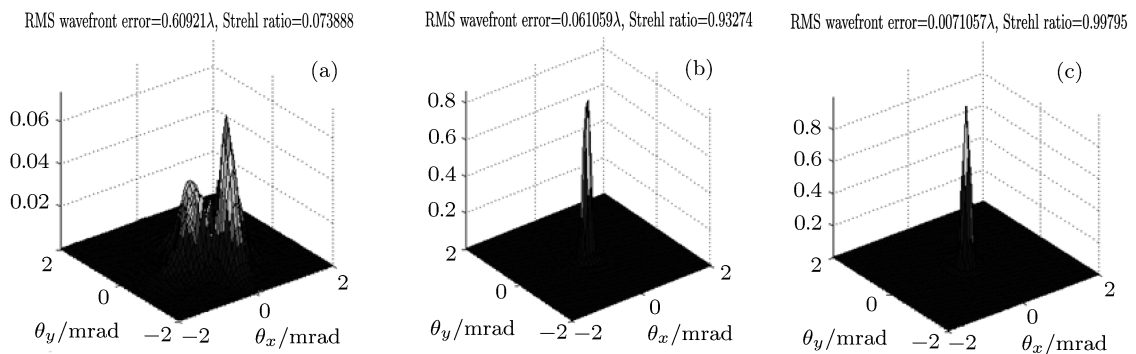


Fig. 7. The PSF (a) before correction; (b) after correction of SNLC AOS; (c) after correction of MNLC AOS. The SRs are 7.39%, 93.24% and 99.80%, respectively.

The residual error of each Zernike mode was analysed. In Fig. 9, we show the dynamic variation of the 1st and 4th Zernike coefficients of residual wavefront. It can be seen that the 1st or the 4th Zernike coefficient of the

residual wavefront corrected by MNLC AOS fluctuated around zero, which is consistent with the expected ideal condition. The result also shows that all of the M Zernike coefficients of the residual wavefront corrected by MNLC AOS fluctuated around zero, which again proves that the gray map reconstruction with mode method is more accurate and suitable for NLC AOS.

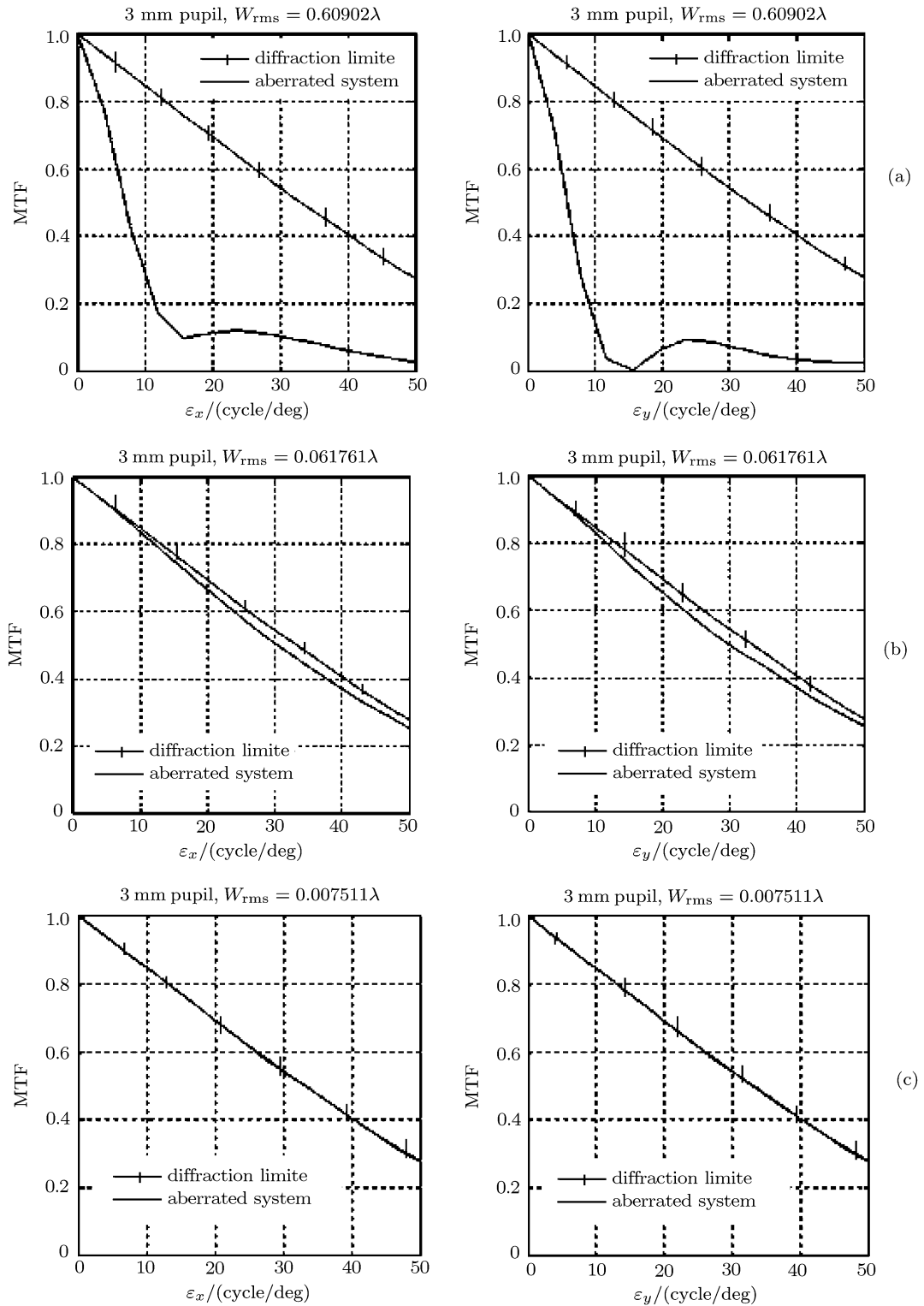


Fig. 8. The MTF in x and y directions: (a) before correction; (b) after correction of SNLC AOS; (c) after correction of MNLC AOS.

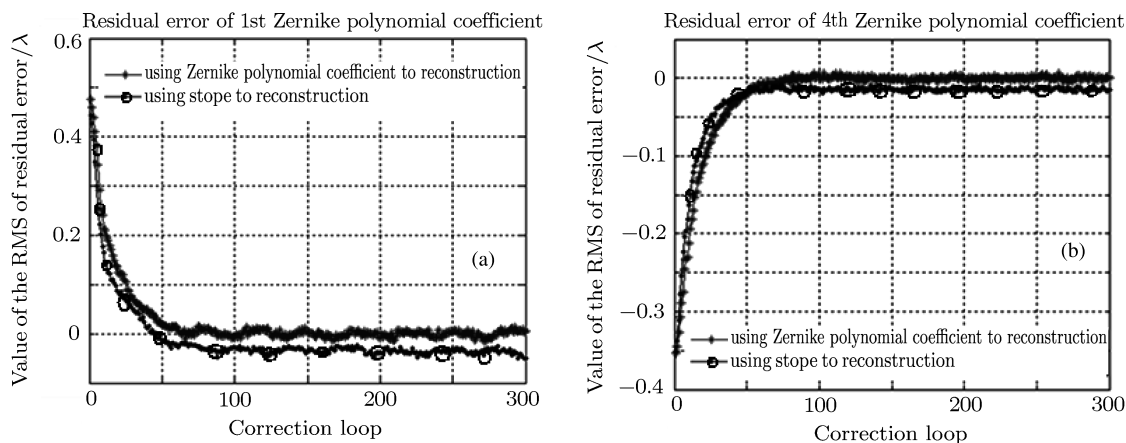


Fig. 9. The dynamic variation of the 1st Zernike coefficient (a) or the 4th Zernike coefficient (b) of the residual wavefront using mode method or slope method in NLC AOS.

5. Conclusion

We demonstrated that aberration correction with mode method has high precision in NLC AOS. Firstly, it was found that the Zernike coefficients of the residual wavefront corrected by slope method in LCAOS do not fluctuate around zero, but with the mode method they do. Secondly, the single loop correction experiment showed that the mode method has a smaller error in gray map reconstruction than the slope method.

Finally, the contrast close-loop correction experiment using the slope method and mode method was conducted to correct static aberration in the laboratory. It was shown that the PV and RMS of the residual wavefront corrected by mode method were nearly one order of magnitude smaller than the ones corrected by slope method. The SR was up to 99.8% through mode method from 7.4%, which was much higher than 93.2% reached through slope method from 7.4%. The MTF was nearly the same as the diffraction limit using mode method, which was much better than the ones using slope method. So we highly recommend the mode method for a reconstructed gray map to correct aberrations in LCAOS.

References

- [1] Ellerbroek B 1994 *J. Opt. Soc. Am. A* **11** 783
- [2] Max C, Olivier S, Friedman H, An J, Avicola K, Beeman B, Bissinger H, Brase J, Erbert G and Gavel D 1997 *Science* **277** 1649
- [3] Van D M, Le M D and Macintosh B 2004 *Appl. Opt.* **43** 5458
- [4] Jiang B G, Cao Z L, Mu Q Q, Li C and Xia M L 2004 *Optics and Precision Engineering* **16** 1805 (in Chinese)
- [5] Chen D, Jones S, Silva D and Olivier S 2007 *J. Opt. Soc. Am. A* **24** 1305
- [6] Jiang B G, Cao Z L, Mu Q Q, Hu L F, Li C and Xuan L 2008 *Chin. Phys. B* **17** 4529
- [7] Porter J, Queener H M, Lin J E, Thorn K and Awwal A 2006 *Adaptive Optics for Vision Science* (New York: John Wiley & Sons) p. 122
- [8] Hu L H, Xuan L, Liu Y G, Cao Z L, Li D Y and Mu Q Q 2004 *Opt. Express* **12** 6403
- [9] Mu Q Q, Cao Z L, Hu L F, Li D Y and Xuan L 2006 *Opt. Express* **14** 8013
- [10] Love G D 1997 *Appl. Opt.* **36** 1517
- [11] Cao Z L, Mu Q Q, Hu L F, Li D Y, Peng Z H, Liu Y G and Xuan L 2009 *Opt. Express* **17** 2530
- [12] Mu Q Q, Cao Z L, Li C, Jiang B G, Hu L F and Xuan L 2008 *Opt. Lett.* **33** 2898
- [13] Li C, Xia M L, Jiang B G, Mu Q Q, Cheng S Y and Xuan L 2009 *Opt. Commun.* **282** 1496
- [14] Mu Q Q, Cao Z L, Li D Y, Hu L F and Xuan L 2008 *Appl. Opt.* **47** 4297
- [15] Thibos L, Applegate R, Schwiegerling J and Webb R 2000 *Vision Science and Its Applications* **35** 232